

1 Estimation of sulfuric acid concentration using ambient ion 2 composition and concentration data obtained by Atmospheric 3 Pressure interface Time-of-Flight ion mass spectrometer

4 Lisa J. Beck¹, Siegfried Schobesberger², Mikko Sipilä¹, Veli-Matti Kerminen^{1,4} and Markku
5 Kulmala^{1,3,4,5}

6 ¹Institute for Atmospheric and Earth System Research/Physics, University of Helsinki, 00014 Helsinki, Finland

7 ²Department of Applied Physics, University of Eastern Finland, 70211 Kuopio, Finland

8 ³Aerosol and Haze Laboratory, Beijing Advanced Innovation Center for Soft Matter Sciences and Engineering,
9 Beijing University of Chemical Technology (BUCT), Beijing, China

10 ⁴Joint International Research Laboratory of Atmospheric and Earth System Sciences, School of Atmospheric
11 Sciences, Nanjing University, Nanjing, China

12 ⁵Faculty of Geography, Lomonosov Moscow State University, Moscow, Russia

13
14 *Correspondence to:* Lisa Beck (lisa.beck@helsinki.fi) and Markku Kulmala (markku.kulmala@helsinki.fi)

15 16 **Abstract**

17 Sulfuric acid (H₂SO₄, SA) is the key compound in atmospheric new particle formation. Therefore, it is crucial to
18 observe its concentration with sensitive instrumentation, such as chemical ionisation (CI) inlets coupled to
19 Atmospheric Pressure interface Time-of-Flight mass spectrometers (APi-TOF). However, there are environmental
20 conditions and physical reasons when chemical ionisation cannot be used, for example in certain remote places
21 or flight measurements with limitations regarding chemicals. Here, we propose a theoretical method to estimate
22 the SA concentration based on ambient ion composition and concentration measurements that are achieved by
23 APi-TOF alone. We derive a theoretical expression to estimate SA concentration and validate it with accurate CI-
24 APi-TOF observations. Our validation shows that the developed estimate works well during daytime in the boreal
25 forest ($R^2 = 0.85$), however it underestimates the SA concentration in e.g. Antarctic atmosphere during new
26 particle formation events where the dominating pathway for nucleation involves sulfuric acid and a base ($R^2 =$
27 0.48).

28 29 30 **1 Introduction**

31 Sulfuric acid (H₂SO₄, SA) is the key compound in atmospheric new particle formation (e.g. Weber et al., 1995,
32 1996; Birmili et al., 2003; Kulmala et al., 2004; Kuang et al., 2008; Kerminen et al., 2010; Wang et al., 2011;
33 Kulmala et al., 2014; Yao et al., 2018; Cai et al., 2021), therefore it is crucial to have accurate observations of its
34 concentration. However, ambient concentrations of H₂SO₄ are low, commonly less than a part per trillion by
35 volume ($\sim 2 \cdot 10^7$ molecules cm⁻³), making it challenging to measure it. During the recent years there have been
36 instrumental developments towards a reliable detection of H₂SO₄ in the atmosphere, particularly via the
37 development of a Chemical Ionisation Atmospheric Pressure interface Time-of-Flight mass spectrometer (CI-

38 APi-TOF, Jokinen et al., 2012), using nitric acid as a reagent ion. Still, the measurement technique with CI-API-
39 TOF is relatively challenging, as a thorough calibration i.e. with sulfuric acid as proposed by Kürten et al. (2012),
40 is needed in order to get reliable numbers. Furthermore, the loss of sulfuric acid to surfaces, such as an inlet, and
41 the correct flow rates must be known and characterised.

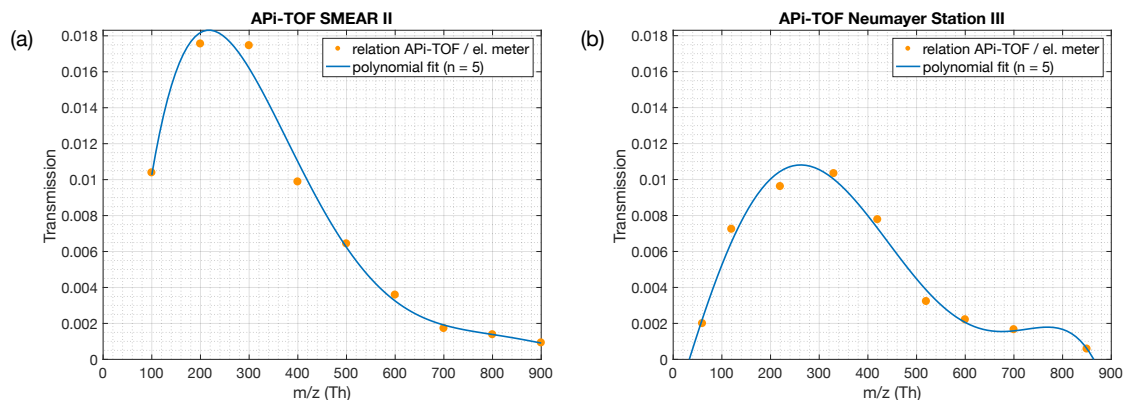
42
43 During the past decade, Atmospheric Pressure interface Time-of-Flight mass spectrometers (APi-TOF, Junninen
44 et al., 2010) have been deployed in several measurement campaigns where the use of a CI inlet was either not
45 possible or desired. In these instances, the APi-TOF only observed the composition and concentration of ambient
46 ions. The APi-TOF is capable of directly sampling and detecting naturally charged gas-phase ions, including
47 molecular clusters, and is often being used to detect clustering processes as a first step of new particle formation
48 on a molecular basis (e.g. Schobesberger et al., 2013; Jokinen et al., 2018; Beck et al., 2021). While a CI-API-
49 TOF at best has a limit of detection of around $\sim 10^4$ molecules cm^{-3} (\sim ppq level), the APi-TOF can detect
50 approximately 1% of the ambient ion concentration (Fig. 1, Junninen et al., 2010). With an average ion
51 concentration of $\sim 1000 \text{ cm}^{-3}$ per polarity (Hirsikko et al., 2011), the APi-TOF is measuring $10 \text{ ions cm}^{-3}\text{s}^{-1}$ with a
52 limit of detection of ~ 0.01 counts per second, hence 0.1 ions cm^{-3} . This corresponds to approximately a pps level
53 ($100 \cdot 10^{-21}$), showing that the limit of detection of an APi-TOF in comparison to a CI-API-TOF is lower by five
54 orders of magnitudes.

55
56 A detailed description of the APi-TOF can be found in Junninen et al. (2010). Since concentrations of neutral
57 clusters are below the detection limit of CI-API-TOF in many atmospheric conditions and environments, using
58 the APi-TOF is currently the only way to directly detect atmospheric clustering. Therefore, if we can estimate
59 H_2SO_4 concentration particularly during initial steps of new particle formation, based on the same dataset, we can
60 readily get better insight into the process itself.

61
62 Since there are only limited long term observations of H_2SO_4 concentrations, several proxies on this concentration
63 have been developed (e.g. Petäjä et al., 2009; Mikkonen et al., 2011; Lu et al., 2019; Dada et al., 2020). These
64 proxies attempt to approximate the ambient H_2SO_4 concentrations using more readily measured quantities, in
65 particular the sulfur dioxide concentration, (UV) radiation intensity and pre-existing particle number size
66 distribution that can be used to calculate the condensation sink for gas-phase H_2SO_4 . In circumstances where the
67 required data for H_2SO_4 proxies are not available, but measurements with an APi-TOF were conducted, the H_2SO_4
68 concentration can be obtained from the ion mass spectra. A first attempt of estimating the sulfuric acid
69 concentration via the concentration of atmospheric ions was introduced by Arnold and Fabian (1980), followed
70 by Eisele (1989) under the assumption that most H_2SO_4 molecules are charged by reacting with NO_3^- .

71
72 Motivated by the reasonings outlined above, we derive here an expression to estimate H_2SO_4 concentration based
73 primarily on APi-TOF observations and validate it.

74
75
76



77

78

79

80

81

82

83

84

Figure 1 Ion transmission of the APi-TOFs used in this study. The transmission efficiency was determined via production of charged particles with a NiCr wire. The concentration of the size selected ions with a Hermann nano differential mobility analyser (HDMA, Hermann, 2000) were measured with an electrometer and an APi-TOF in parallel. A more detailed description can be found in Junninen et al. (2010). Panel (a) shows the transmission efficiency of the APi-TOF used for measurements at the SMEAR II Station, Hyytiälä, Finland. Panel (b) shows the transmission efficiency used for measurements at the Neumayer Station III.

85

2 Theoretical estimation of sulfuric acid concentration with bisulphate ion and H₂SO₄ clusters

86

87

88

89

90

91

92

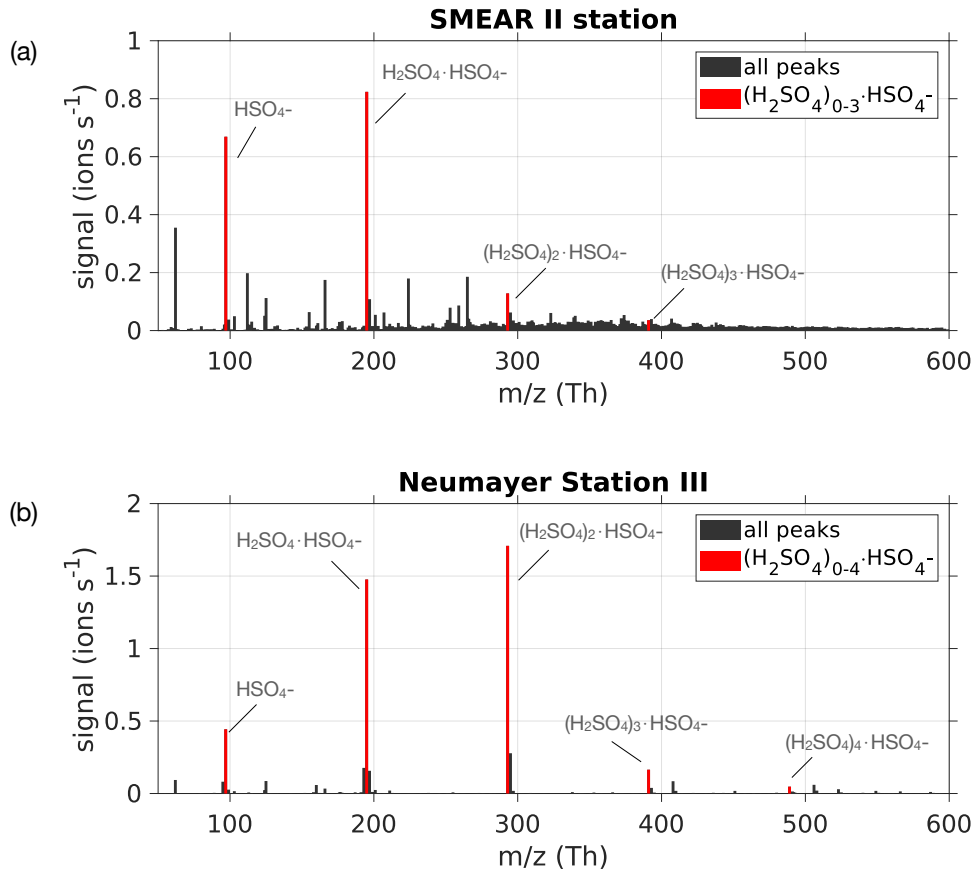
93

94

95

96

Ambient ion mass spectra have usually clear evidence of gas-phase H₂SO₄, predominantly in the form of bisulphate ion (HSO₄⁻) and its adducts involving H₂SO₄, forming so-called dimers (H₂SO₄·HSO₄⁻) as well as larger clusters (Ehn et al., 2010). These ions are due to the efficient scavenging of a negative charge by ambient H₂SO₄ via proton donation, and due to the high stability of the sulfuric acid-bisulphate ion clusters, in particular for the dimer (Ortega et al., 2014). In order to estimate the sulfuric acid concentration (H₂SO₄) using measured naturally charged ions (see Fig. 2), we approximate this concentration by following the bisulphate ion HSO₄⁻, herein denoted SA_{monomer}, the dimer cluster H₂SO₄·HSO₄⁻ (SA_{dimer}) and trimer cluster (H₂SO₄)₂·HSO₄⁻ (SA_{trimer}). Any other H₂SO₄-containing ion clusters, in particular those larger than the SA_{trimer}, typically occur at much smaller concentrations and will be neglected here.



97

98 **Figure 2** (a) Mass spectrum from 50 to 600 Th measured with the API-TOF on 24 May 2017 during the time period 08:00 –
 99 18:00 (local time) at SMEAR II station, Hyytiälä, Finland. (b) Mass spectrum from 14 January 2019 between 08:00 and 18:00
 100 (local time) at Neumayer Station III, Antarctica during a new particle formation event. The bisulphate ion HSO_4^- and H_2SO_4
 101 clusters containing it were used for the estimation of H_2SO_4 concentration, and are coloured in red.

102

103

104 If we assume that the concentration of $\text{SA}_{\text{monomer}}$ depends generally on its production rate (P_1) and that its loss is
 105 by condensation onto aerosol particles (condensation sink, CS), to the SA_{dimer} when clustering with another H_2SO_4
 106 molecule, and to ion-ion recombination with positive ions (N_{pos}), we get the following equation for the $\text{SA}_{\text{monomer}}$
 107 concentration:

108

$$\frac{d[\text{SA}_{\text{monomer}}]}{dt} = P_1 - \text{CS} \cdot [\text{SA}_{\text{monomer}}] - P_2 - \alpha \cdot [\text{SA}_{\text{monomer}}] \cdot N_{\text{pos}}, \quad (1)$$

109

110 where $P_2 = k_1 \times [\text{SA}_{\text{monomer}}] \times [\text{H}_2\text{SO}_4]$ is the dimer production rate due to $\text{SA}_{\text{monomer}}\text{-H}_2\text{SO}_4$ collisions, α (≈ 1.6
 111 $\times 10^{-6} \text{ cm}^3 \text{ s}^{-1}$) is the ion-ion recombination coefficient (Kontkanen et al., 2013), and the collision rate k_1 is assumed
 112 to be constant.

113

114 For the dimer concentration we consider the production P_2 , the loss due to CS, the clustering of the SA_{dimer} with
 115 H_2SO_4 with a rate constant k_2 , and the ion-ion recombination:
 116

$$\frac{d[SA_{dimer}]}{dt} = P_2 - CS \cdot [SA_{dimer}] - k_2 \cdot [SA_{dimer}] \cdot [H_2SO_4] - \alpha \cdot [SA_{dimer}] \cdot N_{pos}, \quad (2)$$

117
 118 And with substituting P_2 , eq. 2 for SA_{dimer} changes to:
 119

$$\frac{d[SA_{dimer}]}{dt} = k_1 \cdot [SA_{monomer}] \cdot [H_2SO_4] - CS \cdot [SA_{dimer}] - k_2 \cdot [SA_{dimer}] \cdot [H_2SO_4] - \alpha \cdot [SA_{dimer}] \cdot N_{pos}. \quad (3)$$

120
 121 Finally, to produce SA_{trimer} we consider the collision of the SA_{dimer} with H_2SO_4 and the loss to the CS and ion-ion
 122 recombination. For the sake of completeness, we would additionally have to consider the loss of $SA_{trimers}$ to form
 123 the tetramer $(H_2SO_4)_3 \cdot HSO_4$, however this additional term is rather small and will therefore be neglected in this
 124 derivation. Therefore, we get the simplified equation for SA_{trimer} :
 125

$$\frac{d[SA_{trimer}]}{dt} = k_2 \cdot [SA_{dimer}] \cdot [H_2SO_4] - CS \cdot [SA_{trimer}] - \alpha \cdot [SA_{trimer}] \cdot N_{pos}. \quad (4)$$

126
 127 For simplification, we consider a pseudo-steady state condition for both dimers and trimers by setting the left-
 128 hand side of eqs. (3) and (4) to be zero, which is justified when the dimer and trimer concentrations change at
 129 rates smaller than their overall production and loss rates. Thereby, from eq. (3) we obtain:
 130

$$k_1 \cdot [SA_{monomer}] \cdot [H_2SO_4] = CS \cdot [SA_{dimer}] + k_2 \cdot [SA_{dimer}] \cdot [H_2SO_4] + \alpha \cdot [SA_{dimer}] \cdot N_{pos} \quad (5)$$

131
 132 and from eq. (4) we obtain:
 133

$$k_2 \cdot [SA_{dimer}] \cdot [H_2SO_4] = CS \cdot [SA_{trimer}] + \alpha \cdot [SA_{trimer}] \cdot N_{pos}. \quad (6)$$

134
 135 If we now deploy equation (6) in equation (5) and solve for H_2SO_4 , the result is:
 136

$$k_1 \cdot [SA_{monomer}] \cdot [H_2SO_4] = CS \cdot [SA_{dimer}] + CS \cdot [SA_{trimer}] + \alpha \cdot [SA_{dimer}] \cdot N_{pos} + \alpha \cdot [SA_{trimer}] \cdot N_{pos}, \quad (7)$$

$$[H_2SO_4] = \frac{(CS + \alpha \cdot N_{pos}) \cdot ([SA_{dimer}] + [SA_{trimer}])}{k_1 \cdot [SA_{monomer}]} \quad (8)$$

137

138 Besides the steady-state assumption, it should be noted that in deriving eq. 8 monomers, dimers and trimers were
 139 assumed to have the same loss rate (CS) onto pre-existing aerosol particles. This causes an additional, yet minor,
 140 uncertainty in the estimated H₂SO₄ concentrations, as such loss rates are dependent on the size/mass of the clusters
 141 (e.g. Lehtinen et al., 2007; Tuovinen et al., 2021). According to Tuovinen et al. (2021), the CS of H₂SO₄ clusters
 142 decreases with increasing number of H₂SO₄ molecules. The study shows that the CS of the SA_{dimer} clustered with
 143 ammonia decreases to 68% (compared to one H₂SO₄ molecule) and for SA_{pentamer} with four ammonia molecules
 144 to 42%. However, the order of magnitude of the CS remains the same, and the effect on the estimation of the
 145 H₂SO₄ concentration is assumed to be negligible. Additionally, the CS for ions is higher than for neutral
 146 compounds. The enhancement of CS has shown to reach a maximum value of 2 when the pre-existing particles
 147 are < 10 nm and decreases to 1 when the pre-existing particles are > 100 nm, as shown by Mahfouz and Donahue
 148 (2021).

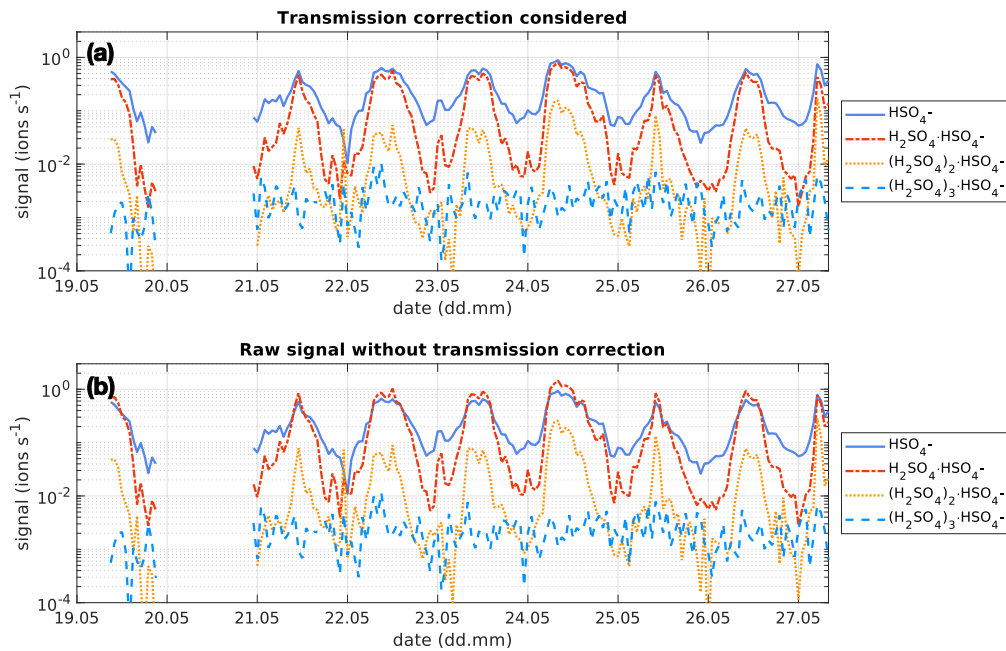
149
 150 Furthermore, the derivation neglects the losses of SA_{trimer} to the SA_{tetramer} and larger clusters, as well as the
 151 clustering of sulfuric acid ion clusters with water and base molecules, such as NH₃. Those simplifications can
 152 cause an underestimation of the H₂SO₄ concentration with the presented method. If necessary, the method can
 153 easily be adapted, and bigger clusters can be included in the equation.

154
 155 From equation 8 we also see that the concentration of H₂SO₄ is proportional to relative concentrations of sulfuric
 156 acid monomers, dimers and trimers clustered with the bisulphate ion:

$$[H_2SO_4] \sim \frac{[SA_{dimer}] + [SA_{trimer}]}{[SA_{monomer}]} \quad (9)$$

158
 159 To estimate the H₂SO₄ concentration with the ion mode APi-TOF, we can therefore use this theoretical approach,
 160 in particular Eq. 8. For the collision rate of H₂SO₄ with HSO₄⁻ we use $k_1 = 2 \cdot 10^{-9} \text{ cm}^3 \text{ molecule}^{-1} \text{ s}^{-1}$ as in Lovejoy
 161 et al. (2004). The value of CS is calculated based on Kulmala et al. (2012). Even if the CS was unknown due, for
 162 example, to the lack of particle measurements, the daytime variability of the H₂SO₄ concentration could still be
 163 estimated by using the relation of the H₂SO₄-containing cluster with HSO₄⁻, as it is proportional to the H₂SO₄
 164 concentration (see eq. 9). If the concentration of positive small ions is not available, it can be assumed to be in the
 165 range of 500 – 1000 cm⁻³ which is a reasonable approximation for the average concentration (Hirsikko et al.,
 166 2011).

167
 168 As the transmission of clusters within an APi-TOF depends on the tuning of the instrument and on the pressures
 169 within its chambers, the transmission efficiency needs to be considered, in order to get reliable concentrations of
 170 the SA_{monomer}, SA_{dimer}, and SA_{trimer}. Fig. 1 shows the transmission efficiency curve of the APi-TOF used at the
 171 SMEAR II station and Neumayer Station III. The effect of applying the transmission correction to the different
 172 SA clusters is depicted in Fig. 3 for the time series at the SMEAR II station. All ion signals were normalised to a
 173 transmission of 1%. As can be determined from Fig. 1a, the SA_{monomer}'s transmission at SMEAR II was ~1%,
 174 while the dimer and trimer were corrected by a factor of 1/1.8 and 1/1.65, respectively. The correction was also
 175 applied on the ions measured at the Neumayer Station III according to the APi-TOF's transmission (Fig. 1b).



177

178 **Figure 3** Time series of the bisulphate ion (HSO_4^- , $\text{SA}_{\text{monomer}}$), H_2SO_4 clustered with bisulphate ($\text{H}_2\text{SO}_4 \cdot \text{HSO}_4^-$, SA_{dimer}), two
 179 H_2SO_4 molecules clustered with the bisulphate ion ($(\text{H}_2\text{SO}_4)_2 \cdot \text{HSO}_4^-$, $\text{SA}_{\text{trimer}}$) and three H_2SO_4 molecules clustered with the
 180 bisulphate ion ($(\text{H}_2\text{SO}_4)_3 \cdot \text{HSO}_4^-$, $\text{SA}_{\text{tetramer}}$) between 19 and 27 May 2017 at SMEAR II station, Hyytiälä, Finland. The
 181 concentration is given in ions s^{-1} as measured by the Api-TOF. The upper panel shows the concentration of the clusters
 182 considering the transmission efficiency of the instrument (see Fig. 1). The lower panel shows the concentration of the clusters
 183 without that correction and assuming a constant transmission efficiency of 1% for all ions.

184

185

186 3 Validation

187 We tested the expression derived above using a dataset collected during inter-comparison measurements at the
 188 SMEAR II station in Hyytiälä, Finland (Hari and Kulmala, 2005). In Fig. 4 we show the time series of the observed
 189 H_2SO_4 concentrations, measured with a CI-API-TOF. The CI-API-TOF was calibrated for sulfuric acid, based on
 190 the method by Kürten et al., (2012) and resulted in a calibration factor of 2.5×10^9 . Additionally, we show the
 191 estimated sulfuric acid concentration based on API-TOF measurements together with Eq. 8 and the sulfuric acid
 192 proxy concentration (Dada et al., 2020). The concentration of positive ions for the estimated sulfuric acid
 193 concentration was obtained from a Neutral cluster and Air Ion Spectrometer (NAIS, Airl Ltd., Mirme and Mirme,
 194 2013).

195

196 The estimated H_2SO_4 concentration agrees with the measured one during most of the daytime. Between 06:00 and
 197 18:00 local time, the correlation (R^2) between the estimated and measured H_2SO_4 concentration is equal to 0.85
 198 with a root mean square error (RMSE) of $4.12 \times 10^5 \text{ cm}^{-3}$. During night-time, the corresponding values are 0.85
 199 and $3.23 \times 10^5 \text{ cm}^{-3}$ (Table 1).

200

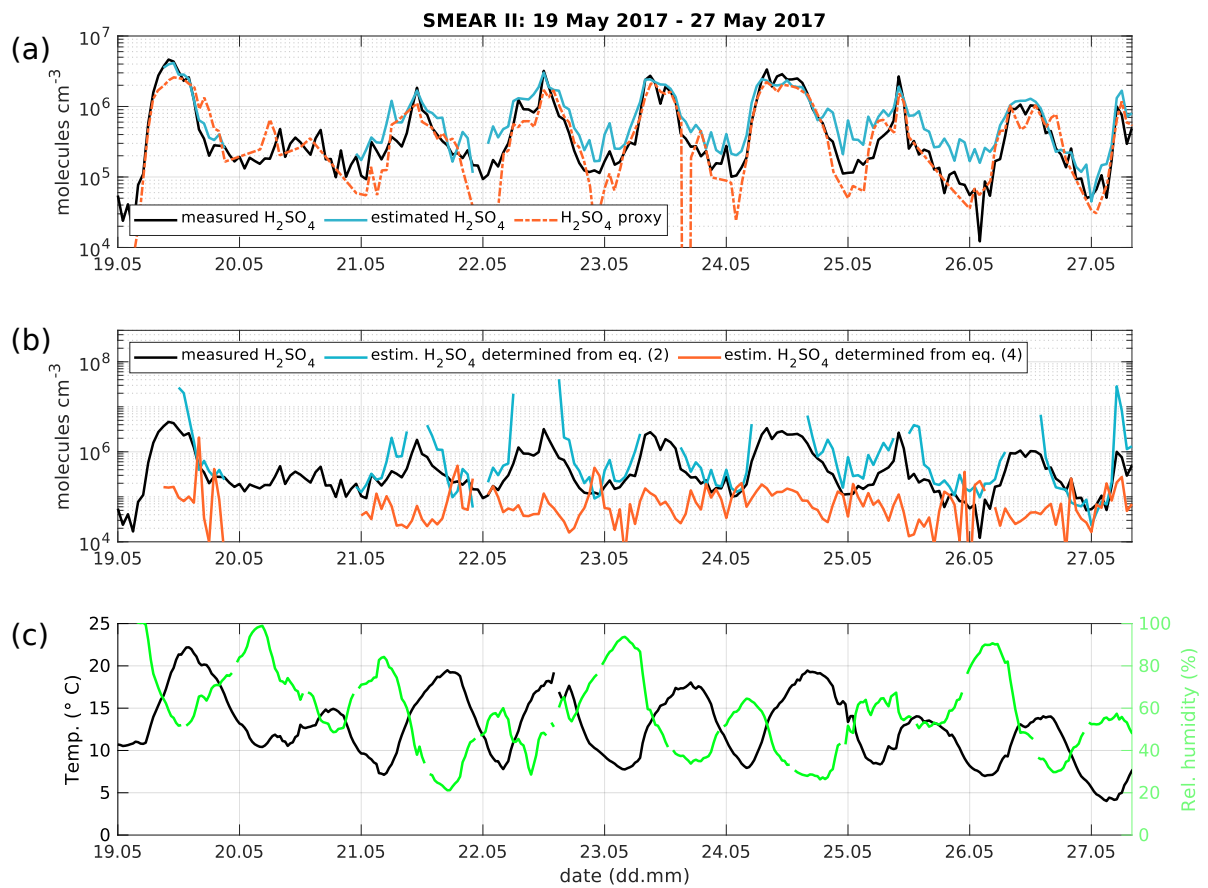
201 The scatter plot in Fig. 5 shows that the estimated H₂SO₄ concentrations agree well with the observed one when
 202 H₂SO₄ concentrations are larger than $2 \times 10^6 \text{ cm}^{-3}$, demonstrating that our method works particularly well at the
 203 SMEAR II station during conditions that favour the formation of H₂SO₄-containing clusters.

204
 205

206 **Table 1:** Root mean square error (RMSE) and R² of the estimated H₂SO₄ concentration at the SMEAR II station and Neumayer
 207 Station III. The day- and night-time are split in 06:00 – 18:00 local time (LT) and 18:00 – 06:00 LT, respectively. For the
 208 SMEAR II station, we also show the RMSE and R² of the H₂SO₄ proxy calculated with the introduced method by (Dada et al.,
 209 2020).

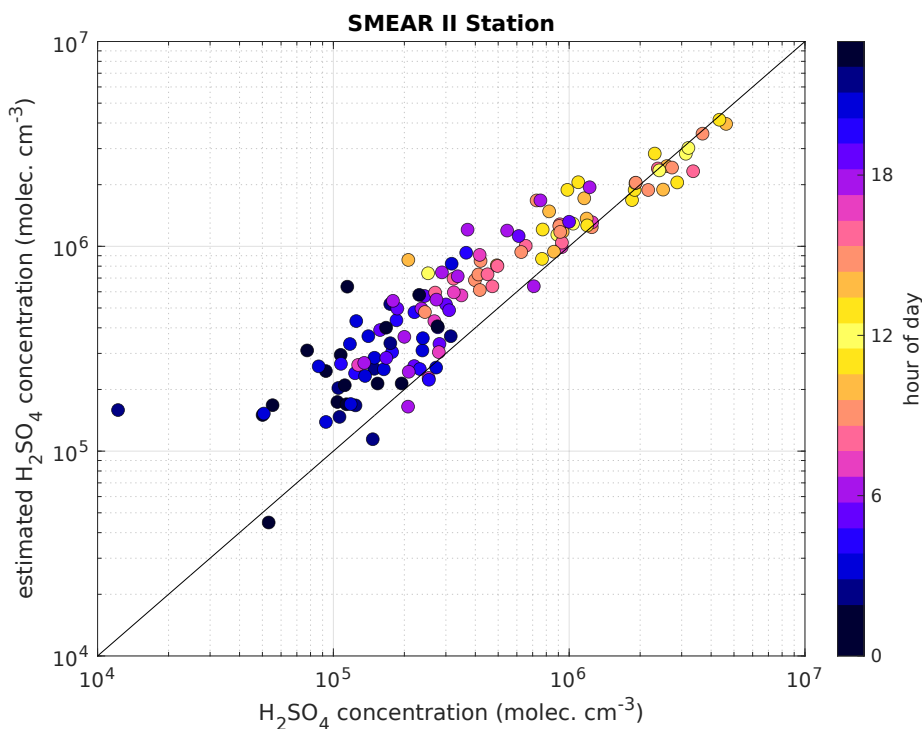
	Root mean square error (RMSE)		
	SMEAR II		Neumayer Station III
	Estimated H ₂ SO ₄ eq. (8)	H ₂ SO ₄ proxy	Estimated H ₂ SO ₄ eq. (8)
Daytime	$4.12 \times 10^5 \text{ cm}^{-3}$	$5.54 \times 10^5 \text{ cm}^{-3}$	$1.43 \times 10^6 \text{ cm}^{-3}$
Night-time	$3.23 \times 10^5 \text{ cm}^{-3}$	$4.25 \times 10^5 \text{ cm}^{-3}$	$1.63 \times 10^6 \text{ cm}^{-3}$
	R ²		
Daytime	0.85	0.78	0.48
Night-time	0.85	0.84	0.37

210
 211



212
 213
 214
 215
 216
 217

Figure 4 (a) Time series of measured H_2SO_4 concentration from the CI-API-TOF (black) and estimated H_2SO_4 concentration from the API-TOF (blue) and H_2SO_4 proxy from Dada et al. (2020) (orange) between 19 and 27 May 2017. The concentration is given in molecules cm^{-3} . (b) Measured H_2SO_4 concentration as in panel (a) in black and determined concentration from eq. 2 (blue) and eq. 4 (orange). (c) Temperature and relative humidity.



218

219 **Figure 5** Measured H_2SO_4 concentration using a CI-API-TOF (horizontal-axis) versus estimated H_2SO_4 concentration based
 220 on API-TOF results (vertical-axis) at SMEAR II station. For the estimation of H_2SO_4 , the transmission efficiency was taken
 221 into account. The colour is indicating the hour of the day and the black line is the 1:1 ratio. Between 08:00 and 16:00 local
 222 time, the concentrations are agreeing well. The shown data contains the time period from 19 to 27 May 2017. The overall
 223 correlation coefficient (Pearson) is 0.94.

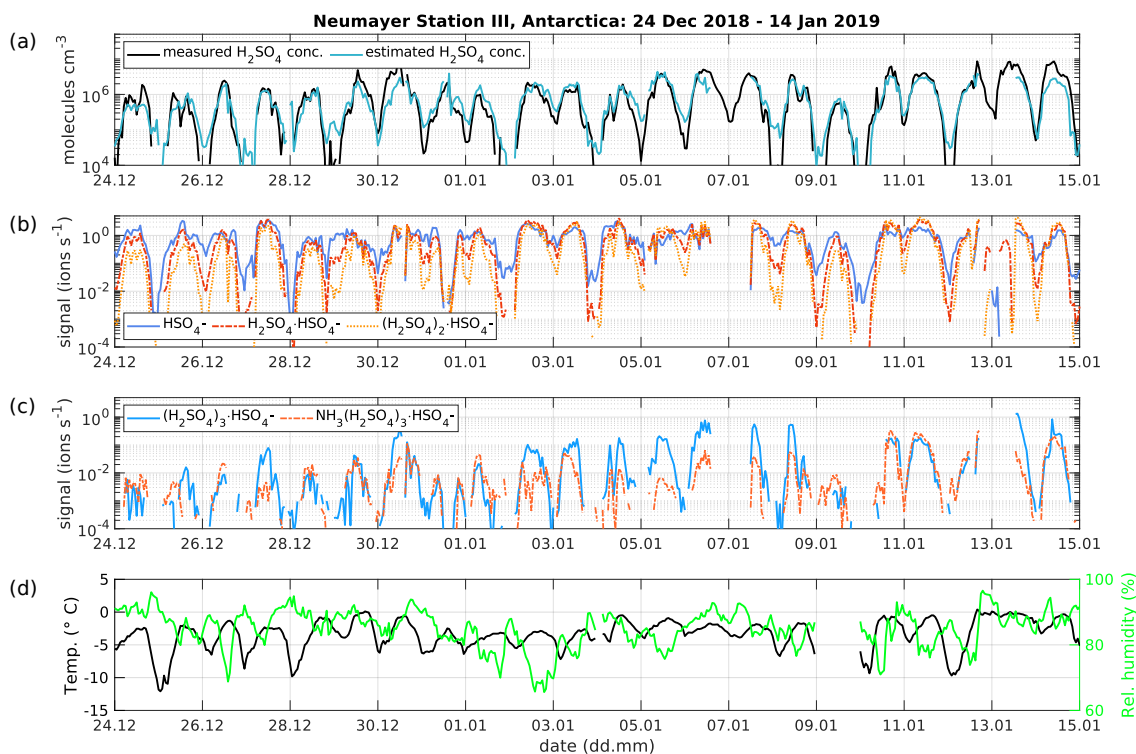
224

225 For the sake of completeness, the estimation of the H_2SO_4 concentration determined from Eqs. 2 and 4, assuming
 226 pseudo-steady state, are depicted in Fig. 4b. The estimated H_2SO_4 concentration from Eq. 2 is highly
 227 overestimating, since the losses of the SA_{dimer} to the $\text{SA}_{\text{trimer}}$ are neglected. When solving Eq. 4 for H_2SO_4 , only
 228 the needed H_2SO_4 for the formation of the trimer is considered and the monomer and dimer production are
 229 neglected. Consequently, the resulting estimated H_2SO_4 concentration is vastly underestimating the real
 230 concentration.

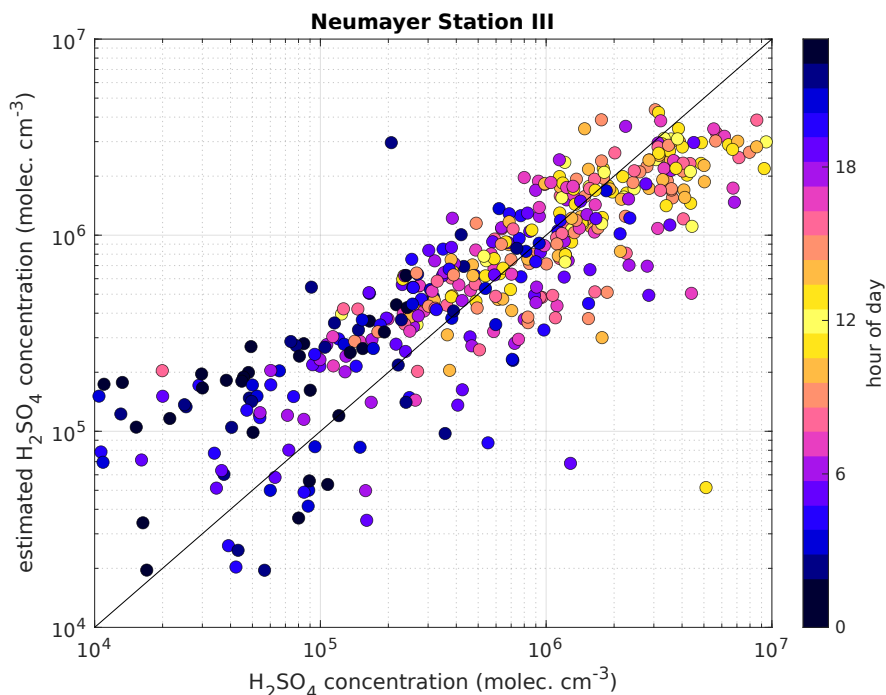
231

232 The presented method was also applied to measurements taken at the Neumayer Station III, Antarctica, in order
 233 to test it in a different environment. Here, we used the condensation sink reported by Weller et al. (2015) at
 234 Neumayer Station of $1 \times 10^{-3} \text{ s}^{-1}$. Figure 6 shows a three-week period between 24 December 2018 and 14 January
 235 2019. The calibration factor of the CI-API-TOF used for measuring the sulfuric acid concentration is 4.9×10^9 .
 236 Here, the estimated sulfuric acid concentration underestimates the measured concentration when the $\text{SA}_{\text{tetramer}}$ and
 237 $\text{NH}_3(\text{H}_2\text{SO}_4)_3\text{HSO}_4$ - cluster show high concentrations (Fig. 6c). A possible explanation for the underestimation
 238 might be the neglect of the growth of sulfuric acid to oligomers larger than the tetramer, as well as its clustering
 239 with bases and water (Fig. 6b and c). In coastal Antarctica, the main nucleating mechanism was observed to be
 240 negative ion-induced sulfuric acid-ammonia nucleation, acting as a major sink for sulfuric acid molecules due to
 241 its clustering with bases (Jokinen et al., 2018). Including the $\text{SA}_{\text{tetramer}}$ and $\text{SA}_{\text{tetramer}}$ clustered with NH_3 in the
 242 estimation equation improved the correlation (R^2) from 0.48 to 0.54. Nevertheless, the diurnal variation of the SA

243 concentration is represented well by this method. During times with lower sulfuric acid concentrations, our
 244 method gives higher values than the measured concentrations (Fig. 6).



245
 246 **Figure 6** (a) Time series of measured H₂SO₄ concentration from the CI-APi-TOF (black) and estimated H₂SO₄ concentration
 247 from the APi-TOF (blue) between 24 December 2018 and 14 January 2019 at Neumayer Station III, Antarctica. The
 248 concentration is given in molecules cm⁻³. (b) Time series of the bisulphate ion (HSO₄⁻, SA_{monomer}), H₂SO₄ clustered with
 249 bisulphate (H₂SO₄·HSO₄⁻, SA_{dimer}), two H₂SO₄ molecules clustered with the bisulphate ion ((H₂SO₄)₂·HSO₄⁻, SA_{trimer}) and (c)
 250 three H₂SO₄ molecules clustered with the bisulphate ion ((H₂SO₄)₃·HSO₄⁻, SA_{tetramer}) as well as the SA_{tetramer} clustered with
 251 NH₃. (d) Temperature and relative humidity measured at Neumayer Station III.
 252



253
 254 **Figure 7** Measured H₂SO₄ concentration using a CI-APi-TOF (horizontal axis) versus estimated H₂SO₄ concentration based
 255 on APi-TOF results (vertical axis) at the Neumayer Station III. For the estimation of H₂SO₄, the transmission efficiency was
 256 taken into account. The colour is indicating the hour of the day and the black line is the 1:1 ratio. The shown data contains the
 257 time period from 24 December 2016 to 14 January 2019. The overall correlation coefficient (Pearson) is 0.77.
 258

259
 260 **4 Conclusions**

261 Here we derived a theoretical expression to estimate H₂SO₄ concentrations based on APi-TOF measurements of
 262 ambient ions. The estimation agrees well with the measured concentration during daytime in the boreal forest (R²
 263 = 0.85), indicating that the estimation is able to represent the diurnal variation and trend of H₂SO₄ concentrations
 264 during most of the time when active clustering of sulfuric acid is inducing the initial step(s) of atmospheric new
 265 particle formation. However, in an atmosphere, where sulfuric acid is the dominating pathway for initiating new
 266 particle formation, the method might underestimate the H₂SO₄ concentrations, as this method does not include the
 267 rapid clustering to bigger of sulfuric acid clusters and clustering with bases directly, e.g. in the Antarctic
 268 atmosphere (R² = 0.48; during daytime).
 269

270 The APi-TOF's "ion mode", i.e. direct ion sampling without chemical ionisation, remains a crucial tool in many
 271 field deployments and laboratory studies, since it is extremely sensitive and allows for observing atmospheric
 272 clustering molecule by molecule, which in most cases is impossible when relying on chemical ionization.
 273 Therefore, having available a reliable estimate of H₂SO₄ concentration allows us to utilise the APi-TOF ion mode
 274 even more effectively.
 275

276
 277 **Data availability**

278 The data can be accessed via Zenodo (10.5281/zenodo.5266313).

279

280 **Author contribution**

281 LJB, SS, VMK and MK designed the study. LJB and MS performed the measurements. SS and LJB derived the
282 equations. LJB processed and analysed the data and performed the data visualisation. MK and VMK supervised
283 the process. All authors commented and edited the paper.

284

285 **Competing interests**

286 The authors declare that they have no conflict of interest.

287

288 **Acknowledgements**

289 We acknowledge the following projects: ACCC Flagship funded by the Academy of Finland grant number
290 337549, Academy professorship funded by the Academy of Finland (grant no. 302958), Academy of Finland
291 projects no. 1325656, 310682, 316114, 325647 and 296628 , Russian Mega Grant project “Megapolis - heat and
292 pollution island: interdisciplinary hydroclimatic, geochemical and ecological analysis” application reference
293 2020-220-08-5835, “Quantifying carbon sink, CarbonSink+ and their interaction with air quality” INAR project
294 funded by Jane and Aatos Erkkö Foundation, European Research Council (ERC) project ATM-GTP Contract No.
295 742206 and GASPARCON, grant agreement no. 714621. We thank the tofTools team for providing the tools for
296 the mass spectrometry analysis. We thank the technical and scientific staff in Hyytiälä SMEAR II and the
297 technicians and scientists of the Neumayer overwintering teams of the years 2018 and 2019. We thank Lubna
298 Dada for calculating the SA proxy for SMEAR II station. We thank Janne Lampilahti for providing the codes to
299 process the NAIS dataset.

300 **References**

- 301 Arnold, F. and Fabian, R.: First measurements of gas phase sulphuric acid in the stratosphere, 283, 55–57,
302 <https://doi.org/10.1038/283055a0>, 1980.
- 303 Beck, L. J., Sarnela, N., Junninen, H., Hoppe, C. J. M., Garmash, O., Bianchi, F., Riva, M., Rose, C., Peräkylä,
304 O., Wimmer, D., Kausiala, O., Jokinen, T., Ahonen, L., Mikkilä, J., Hakala, J., He, X.-C., Kontkanen, J., Wolf,
305 K. K. E., Cappelletti, D., Mazzola, M., Traversi, R., Petroselli, C., Viola, A. P., Vitale, V., Lange, R., Massling,
306 A., Nøjgaard, J. K., Krejci, R., Karlsson, L., Zieger, P., Jang, S., Lee, K., Vakkari, V., Lampilahti, J., Thakur, R.
307 C., Leino, K., Kangasluoma, J., Duplissy, E.-M., Siivola, E., Marbouti, M., Tham, Y. J., Saiz-Lopez, A., Petäjä,
308 T., Ehn, M., Worsnop, D. R., Skov, H., Kulmala, M., Kerminen, V.-M., and Sipilä, M.: Differing Mechanisms
309 of New Particle Formation at Two Arctic Sites, *Geophysical Research Letters*, 48,
310 <https://doi.org/10.1029/2020GL091334>, 2021.
- 311 Birmili, W., Berresheim, H., Plass-Dülmer, C., Elste, T., Gilge, S., Wiedensohler, A., and Uhrner, U.: The
312 Hohenpeissenberg aerosol formation experiment (HAFEX): a long-term study including size-resolved aerosol,
313 H₂SO₄, OH, and monoterpenes measurements, 3, 361–376, <https://doi.org/10.5194/acp-3-361-2003>, 2003.
- 314 Cai, R., Yan, C., Yang, D., Yin, R., Lu, Y., Deng, C., Fu, Y., Ruan, J., Li, X., Kontkanen, J., Zhang, Q.,
315 Kangasluoma, J., Ma, Y., Hao, J., Worsnop, D. R., Bianchi, F., Paasonen, P., Kerminen, V.-M., Liu, Y., Wang,
316 L., Zheng, J., Kulmala, M., and Jiang, J.: Sulfuric acid–amine nucleation in urban Beijing, 21, 2457–2468,
317 <https://doi.org/10.5194/acp-21-2457-2021>, 2021.
- 318 Dada, L., Ylivinkka, I., Baalbaki, R., Li, C., Guo, Y., Yan, C., Yao, L., Sarnela, N., Jokinen, T., Daellenbach, K.
319 R., Yin, R., Deng, C., Chu, B., Nieminen, T., Wang, Y., Lin, Z., Thakur, R. C., Kontkanen, J., Stolzenburg, D.,
320 Sipilä, M., Hussein, T., Paasonen, P., Bianchi, F., Salma, I., Weidinger, T., Pikridas, M., Sciare, J., Jiang, J.,
321 Liu, Y., Petäjä, T., Kerminen, V.-M., and Kulmala, M.: Sources and sinks driving sulfuric acid concentrations in
322 contrasting environments: implications on proxy calculations, 20, 11747–11766, <https://doi.org/10.5194/acp-20-11747-2020>, 2020.
- 324 Ehn, M., Junninen, H., Petäjä, T., Kurtén, T., Kerminen, V.-M., Schobesberger, S., Manninen, H. E., Ortega, I.
325 K., Vehkamäki, H., Kulmala, M., and Worsnop, D. R.: Composition and temporal behavior of ambient ions in
326 the boreal forest, 10, 8513–8530, <https://doi.org/10.5194/acp-10-8513-2010>, 2010.
- 327 Eisele, F. L.: Natural and anthropogenic negative ions in the troposphere, 94, 2183–2196,
328 <https://doi.org/10.1029/JD094iD02p02183>, 1989.
- 329 Hari, P. and Kulmala, M.: Station for Measuring Ecosystem–Atmosphere Relations (SMEAR II), *Bor. Env.*
330 *Res.*, 10, 315–322, 2005.
- 331 Herrmann, W., Eichler, T., Bernardo, N., and Fernandez de la Mora, J.: Turbulent transition arises at Re 35 000
332 in a short Vienna type DMA with a large laminarizing inlet, *Proceedings of the annual conference of the*
333 *AAAR*, St. Louis, MO, 6–10 October 2000.
- 334
335 Hirsikko, A., Nieminen, T., Gagné, S., Lehtipalo, K., Manninen, H. E., Ehn, M., Hörrak, U., Kerminen, V.-M.,
336 Laakso, L., McMurry, P. H., Mirme, A., Mirme, S., Petäjä, T., Tammet, H., Vakkari, V., Vana, M., and
337 Kulmala, M.: Atmospheric ions and nucleation: a review of observations, 11, 767–798,
338 <https://doi.org/10.5194/acp-11-767-2011>, 2011.
- 339 Jokinen, T., Sipilä, M., Junninen, H., Ehn, M., Lönn, G., Hakala, J., Petäjä, T., Mauldin III, R. L., Kulmala, M.,
340 and Worsnop, D. R.: Atmospheric sulphuric acid and neutral cluster measurements using CI-API-TOF, 12,
341 4117–4125, <https://doi.org/10.5194/acp-12-4117-2012>, 2012.
- 342 Jokinen, T., Sipilä, M., Kontkanen, J., Vakkari, V., Tisler, P., Duplissy, E.-M., Junninen, H., Kangasluoma, J.,
343 Manninen, H. E., Petäjä, T., Kulmala, M., Worsnop, D. R., Kirkby, J., Virkkula, A., and Kerminen, V.-M.: Ion-
344 induced sulfuric acid–ammonia nucleation drives particle formation in coastal Antarctica, *Sci Adv*, 4,
345 <https://doi.org/10.1126/sciadv.aat9744>, 2018.

- 346 Junninen, H., Ehn, M., Petäjä, T., Luosujärvi, L., Kotiaho, T., Kostiaainen, R., Rohner, U., Gonin, M., Fuhrer, K.,
347 Kulmala, M., and Worsnop, D. R.: A high-resolution mass spectrometer to measure atmospheric ion
348 composition, 3, 1039–1053, <https://doi.org/10.5194/amt-3-1039-2010>, 2010.
- 349 Kerminen, V.-M., Petäjä, T., Manninen, H. E., Paasonen, P., Nieminen, T., Sipilä, M., Junninen, H., Ehn, M.,
350 Gagné, S., Laakso, L., Riipinen, I., Vehkamäki, H., Kurten, T., Ortega, I. K., Dal Maso, M., Brus, D.,
351 Hyvärinen, A., Lihavainen, H., Leppä, J., Lehtinen, K. E. J., Mirme, A., Mirme, S., Hörrak, U., Berndt, T.,
352 Stratmann, F., Birmili, W., Wiedensohler, A., Metzger, A., Dommen, J., Baltensperger, U., Kiendler-Scharr, A.,
353 Mentel, T. F., Wildt, J., Winkler, P. M., Wagner, P. E., Petzold, A., Minikin, A., Plass-Dülmer, C., Pöschl, U.,
354 Laaksonen, A., and Kulmala, M.: Atmospheric nucleation: highlights of the EUCAARI project and future
355 directions, 10, 10829–10848, <https://doi.org/10.5194/acp-10-10829-2010>, 2010.
- 356 Kontkanen, J., Lehtinen, K. E. J., Nieminen, T., Manninen, H. E., Lehtipalo, K., Kerminen, V.-M., and Kulmala,
357 M.: Estimating the contribution of ion–ion recombination to sub-2 nm cluster concentrations from atmospheric
358 measurements, 13, 11391–11401, <https://doi.org/10.5194/acp-13-11391-2013>, 2013.
- 359 Kuang, C., McMurry, P. H., McCormick, A. V., and Eisele, F. L.: Dependence of nucleation rates on sulfuric
360 acid vapor concentration in diverse atmospheric locations, 113, <https://doi.org/10.1029/2007JD009253>, 2008.
- 361 Kulmala, M., Vehkamäki, H., Petäjä, T., Dal Maso, M., Lauri, A., Kerminen, V.-M., Birmili, W., and McMurry,
362 P. H.: Formation and growth rates of ultrafine atmospheric particles: a review of observations, *Journal of*
363 *Aerosol Science*, 35, 143–176, <https://doi.org/10.1016/j.jaerosci.2003.10.003>, 2004.
- 364 Kulmala, M., Petäjä, T., Nieminen, T., Sipilä, M., Manninen, H. E., Lehtipalo, K., Dal Maso, M., Aalto, P. P.,
365 Junninen, H., Paasonen, P., Riipinen, I., Lehtinen, K. E. J., Laaksonen, A., and Kerminen, V.-M.: Measurement
366 of the nucleation of atmospheric aerosol particles, 7, 1651–1667, <https://doi.org/10.1038/nprot.2012.091>, 2012.
- 367 Kulmala, M., Petäjä, T., Ehn, M., Thornton, J., Sipilä, M., Worsnop, D. R., and Kerminen, V.-M.: Chemistry of
368 Atmospheric Nucleation: On the Recent Advances on Precursor Characterization and Atmospheric Cluster
369 Composition in Connection with Atmospheric New Particle Formation, 65, 21–37,
370 <https://doi.org/10.1146/annurev-physchem-040412-110014>, 2014.
- 371 Kürten, A., Rondo, L., Ehrhart, S., and Curtius, J.: Calibration of a Chemical Ionization Mass Spectrometer for
372 the Measurement of Gaseous Sulfuric Acid, *J. Phys. Chem. A*, 116, 6375–6386,
373 <https://doi.org/10.1021/jp212123n>, 2012.
- 374 Lehtinen, K. E. J., Dal Maso, M., Kulmala, M., and Kerminen, V.-M.: Estimating nucleation rates from apparent
375 particle formation rates and vice versa: Revised formulation of the Kerminen–Kulmala equation, *Journal of*
376 *Aerosol Science*, 38, 988–994, <https://doi.org/10.1016/j.jaerosci.2007.06.009>, 2007.
- 377 Lovejoy, E. R., Curtius, J., and Froyd, K. D.: Atmospheric ion-induced nucleation of sulfuric acid and water,
378 109, <https://doi.org/10.1029/2003JD004460>, 2004.
- 379 Lu, Y., Yan, C., Fu, Y., Chen, Y., Liu, Y., Yang, G., Wang, Y., Bianchi, F., Chu, B., Zhou, Y., Yin, R.,
380 Baalbaki, R., Garmash, O., Deng, C., Wang, W., Liu, Y., Petäjä, T., Kerminen, V.-M., Jiang, J., Kulmala, M.,
381 and Wang, L.: A proxy for atmospheric daytime gaseous sulfuric acid concentration in urban Beijing, 19, 1971–
382 1983, <https://doi.org/10.5194/acp-19-1971-2019>, 2019.
- 383 Mahfouz, N. G. A. and Donahue, N. M.: Technical note: The enhancement limit of coagulation scavenging of
384 small charged particles, 21, 3827–3832, <https://doi.org/10.5194/acp-21-3827-2021>, 2021.
- 385 Mikkonen, S., Romakkaniemi, S., Smith, J. N., Korhonen, H., Petäjä, T., Plass-Duelmer, C., Boy, M., McMurry,
386 P. H., Lehtinen, K. E. J., Joutsensaari, J., Hamed, A., Mauldin III, R. L., Birmili, W., Spindler, G., Arnold, F.,
387 Kulmala, M., and Laaksonen, A.: A statistical proxy for sulphuric acid concentration, 11, 11319–11334,
388 <https://doi.org/10.5194/acp-11-11319-2011>, 2011.
- 389 Mirme, S. and Mirme, A.: The mathematical principles and design of the NAIS – a spectrometer for the
390 measurement of cluster ion and nanometer aerosol size distributions, 6, 1061–1071, <https://doi.org/10.5194/amt-6-1061-2013>, 2013.

- 392 Ortega, I. K., Olenius, T., Kupiainen-Määttä, O., Loukonen, V., Kurtén, T., and Vehkamäki, H.: Electrical
 393 charging changes the composition of sulfuric acid–ammonia/dimethylamine clusters, 14, 7995–8007,
 394 <https://doi.org/10.5194/acp-14-7995-2014>, 2014.
- 395 Petäjä, T., Mauldin, I. I. I., Kosciuch, E., McGrath, J., Nieminen, T., Paasonen, P., Boy, M., Adamov, A.,
 396 Kotiaho, T., and Kulmala, M.: Sulfuric acid and OH concentrations in a boreal forest site, 9, 7435–7448,
 397 <https://doi.org/10.5194/acp-9-7435-2009>, 2009.
- 398 Schobesberger, S., Junninen, H., Bianchi, F., Lönn, G., Ehn, M., Lehtipalo, K., Dommen, J., Ehrhart, S., Ortega,
 399 I. K., Franchin, A., Nieminen, T., Riccobono, F., Hutterli, M., Duplissy, J., Almeida, J., Amorim, A.,
 400 Breitenlechner, M., Downard, A. J., Dunne, E. M., Flagan, R. C., Kajos, M., Keskinen, H., Kirkby, J., Kupc, A.,
 401 Kürten, A., Kurtén, T., Laaksonen, A., Mathot, S., Onnela, A., Praplan, A. P., Rondo, L., Santos, F. D.,
 402 Schallhart, S., Schnitzhofer, R., Sipilä, M., Tomé, A., Tsagkogeorgas, G., Vehkamäki, H., Wimmer, D.,
 403 Baltensperger, U., Carslaw, K. S., Curtius, J., Hansel, A., Petäjä, T., Kulmala, M., Donahue, N. M., and
 404 Worsnop, D. R.: Molecular understanding of atmospheric particle formation from sulfuric acid and large
 405 oxidized organic molecules, PNAS, 110, 17223–17228, <https://doi.org/10.1073/pnas.1306973110>, 2013.
- 406 Tuovinen, S., Kontkanen, J., Cai, R., and Kulmala, M.: Condensation sink of atmospheric vapors: the effect of
 407 vapor properties and the resulting uncertainties, Environ. Sci.: Atmos., 1, 543–557,
 408 <https://doi.org/10.1039/D1EA00032B>, 2021.
- 409 Wang, Z. B., Hu, M., Yue, D. L., Zheng, J., Zhang, R. Y., Wiedensohler, A., Wu, Z. J., Nieminen, T., and Boy,
 410 M.: Evaluation on the role of sulfuric acid in the mechanisms of new particle formation for Beijing case, 11,
 411 12663–12671, <https://doi.org/10.5194/acp-11-12663-2011>, 2011.
- 412 Weber, R. J., McMurry, P. H., Eisele, F. L., and Tanner, D. J.: Measurement of Expected Nucleation Precursor
 413 Species and 3–500-nm Diameter Particles at Mauna Loa Observatory, Hawaii, 52, 2242–2257,
 414 [https://doi.org/10.1175/1520-0469\(1995\)052](https://doi.org/10.1175/1520-0469(1995)052), 1995.
- 415 Weber, R. J., Marti, J. J., McMurry, P. H., Eisele, F. L., Tanner, D. J., and Jefferson, A.: Measured Atmospheric
 416 New Particle Formation Rates: Implications for Nucleation Mechanisms, 151, 53–64,
 417 <https://doi.org/10.1080/00986449608936541>, 1996.
- 418 Weller, R., Schmidt, K., Teinilä, K., and Hillamo, R.: Natural new particle formation at the coastal Antarctic site
 419 Neumayer, 15, 11399–11410, <https://doi.org/10.5194/acp-15-11399-2015>, 2015.
- 420 Yao, L., Garmash, O., Bianchi, F., Zheng, J., Yan, C., Kontkanen, J., Junninen, H., Mazon, S. B., Ehn, M.,
 421 Paasonen, P., Sipilä, M., Wang, M., Wang, X., Xiao, S., Chen, H., Lu, Y., Zhang, B., Wang, D., Fu, Q., Geng,
 422 F., Li, L., Wang, H., Qiao, L., Yang, X., Chen, J., Kerminen, V.-M., Petäjä, T., Worsnop, D. R., Kulmala, M.,
 423 and Wang, L.: Atmospheric new particle formation from sulfuric acid and amines in a Chinese megacity, 361,
 424 278–281, <https://doi.org/10.1126/science.aao4839>, 2018.
- 425